THE ASTROPHYSICAL JOURNAL, 294:441–454, 1985 July 15

COMPOSITION OF COSMIC-RAY NUCLEI FROM BORON TO NICKEL FOR 1200 TO 2400 MeV PER NUCLEON[1]

ROBERT DWYER AND PETER MEYER[2]
Enrico Fermi Institute, University of Chicago
Received 1984 December 11; accepted 1985 January 28

ABSTRACT

In a series of high-altitude balloon flights we have measured the relative abundances of cosmic-ray nuclei in the charge range boron through nickel ($5 \leq Z \leq 28$) with energies 1200–2400 MeV per nucleon. The instrument is a scintillation and Cerenkov counter telescope with a multiwire proportional chamber hodoscope. Good charge separation ($\sigma \approx 0.2$ charge units at iron) and high statistical accuracy (exposure factor $= 38$ m^{2}sr hr) have been achieved. Implications of these chemical composition measurements for the propagation and path length distribution of cosmic rays as well as the source abundances are discussed.

Subject headings: cosmic rays: abundances — particle acceleration

I. INTRODUCTION

The nuclear composition of cosmic rays plays a significant role in defining both the origin and acceleration of these high-energy particles and their subsequent propagation in the Galaxy. Since the time when nuclei heavier than protons were discovered in the radiation (Freier *et al.* 1948; Bradt and Peters 1948) much effort has been made to unravel the information contained in the nuclear abundances and their energy dependences. One of the major breakthroughs in modern astrophysics was the determination of the element abundance distribution in the cosmic rays, and its comparison with solar system abundances. A steady sequence of refinements in detectors and instruments has made great advances possible and has recently led to the ability to measure even isotopic abundances for individual elements.

Composition measurements at energies >1 GeV per nucleon (GeV n^{-1}) could be made only recently. They are important because of the minimal role played by several interfering effects, which at lower energies must be taken into account and corrected for. Extrapolation of abundances measured at Earth to the nearby interstellar medium requires a knowledge of the influence of solar modulation. This modulation of the incoming particle fluxes is strongly energy dependent, its effects decreasing rapidly with increasing energy, becoming negligible beyond a few GeV n^{-1}. Further, extrapolation from the vicinity of the solar system is needed to determine the abundances at the sources of the cosmic rays, and this requires an understanding of cosmic-ray transport and propagation in the interstellar medium. Two important aspects of this process are energy loss of the cosmic rays by ionization of the medium and spallation of the particles on the interstellar gas. Ionization energy loss represents a decreasing fraction of particle energy for increasing energies which considerably simplifies calculations to account for cosmic-ray transport. The spallation cross sections which are needed to account for the loss of primary and the production of secondary nuclei exhibit considerable energy dependence at lower energy, but become largely energy independent above 1–2 GeV n^{-1} (Lindstrom *et al.* 1975; Heckman *et al.* 1972).

The results that we shall present and discuss here were obtained with a balloon-borne instrument of a design that is aimed at optimal resolution between individual nuclear species over the charge range from boron through nickel ($Z = 5$–28) and at energies of ~ 1 GeV n^{-1}. These results have been obtained in a series of four high-altitude balloon flights from Texas and Oklahoma. While the energy range that can be covered with this instrument extends from below 1 to ~ 10 GeV n^{-1}, we have here restricted the analysis to that interval of energy where the charge and energy resolution is optimal: 1200–2400 MeV n^{-1}. It is important to emphasize that in this interval our data analysis requires, first, no charge overlap corrections whatsoever between adjacent element distributions and, second, no energy deconvolution corrections either. Because of the long exposure times and large size of the instrument, good statistical accuracy is still maintained. The energy spectra of the individual nuclear species over the extended energy range will be the subject of a later paper.

Previous results reported from this experiment include measurements of the isotopic composition of boron through silicon ($Z = 5$–14) at 1.2 GeV n^{-1}, (Dwyer 1978; Dwyer and Meyer 1979) and on the energy spectra of iron and nickel (Minagawa 1981). Preliminary results on the relative elemental abundances were presented at the Paris cosmic-ray conference (Dwyer and Meyer 1981). We now discuss the final analysis of this work and its implications for interstellar propagation and the cosmic-ray source composition (see also Dwyer *et al.* 1981). Particular attention is paid to the problem of the time delay between nucleosynthesis of cosmic-ray matter and its acceleration to high energies.

II. INSTRUMENTATION AND BALLOON FLIGHTS

The instrument that provides the data has been flown in two configurations: the original one in two flights from Palestine, Texas, and a modified version in two flights from Muskogee, Oklahoma. The original version is described in Dwyer (1978); both configurations, with emphasis on the second, are described in Dwyer, Jordan, and Meyer (1984). The second configuration is shown in Figure 1; information on the detectors is given in Table 1.

[1] This work was supported in part by the National Aeronautics and Space Administration under contract NGL-14-001-005.
[2] Department of Physics, University of Chicago.

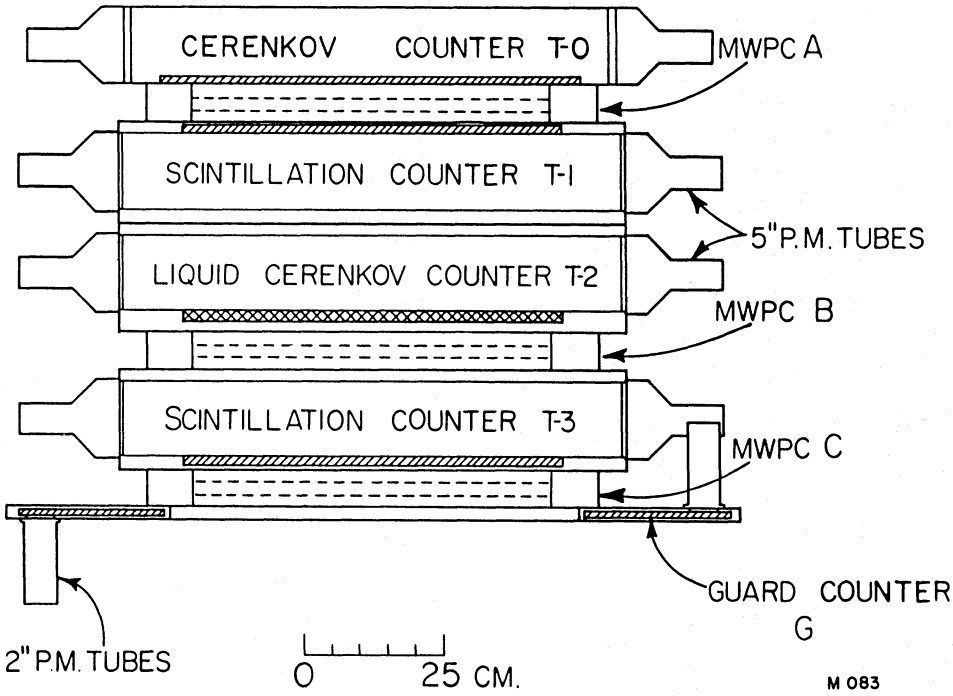

FIG. 1.—Schematic cross section of the instrument. MWPC is multiwire proportional chamber.

The three main modifications made to the original configuration are as follows: (1) The addition of the plastic Cerenkov counter T0 made of Pilot 425 (refractive index $n = 1.49$). The dimensions of the radiator were chosen as to not reduce the telescope opening angle; thus the geometry factor is 0.25 m^2sr for original and modified versions. The counter T0 is used mainly in the charge determination for the analysis presented in this paper. (2) The reduction in thickness of the liquid Cerenkov counter T2 so that the total grammage in the instrument in both versions remained the same after adding T0. (3) The discriminator threshold on each wire in the multiwire proportional chamber (MWPC) hodoscope was increased to a level of 35–40 times that of a minimum ionizing singly charged particle. This led to essentially 100% efficiency for straight-line track selection over the charge range from oxygen through nickel ($Z = 8$–28) in the modified version.

The abundances for B, C, and N relative to oxygen ($Z = 5$–8) presented in this paper are from the Texas flights of the original version, and the abundances for oxygen through nickel are from the Oklahoma flights of the modified version. We have done extensive checks on the data to assure that this combination does not show any systematic bias due to slightly different data analysis procedures for the two instrument versions.

The liquid Cerenkov radiator T2 is filled with Dupont freon fluorocarbon type E-2 with index of refraction $n = 1.270$ suitable for measuring energies from $\sim$0.7 GeV n^{-1} to beyond 8 GeV n^{-1}. This liquid has a refractive index such that its

TABLE 1

DECTECTOR SPECIFICATIONS

DETECTOR	TYPE	THICKNESS 1 (cm)	THICKNESS 2 (g cm^{-2})
T0	Pilot 425 plastic	1.1[a]	1.3[a]
T1	Pilot Y plastic scintillator	1.0	1.0
T2	Dupont freon fluorocarbon liquid type E-2 Cerenkov radiator	2.5[b]	4.2[b]
		1.9[a]	3.2[a]
T3	Pilot Y plastic scintillator	1.0	1.0
G	NE 110 plastic scintillator	0.7	0.7
MWPC, A, B, C hodoscope	Multiwire proportional chamber Ar-Co_2 (80%–20%)	5.0 each	<0.1

NOTE.—Geometry factor = 2500 cm^2 sr. Total power requirement = 52 watts. Total weight of instrument including pressure shell = 1050 kg.

[a] In later configuration (Oklahoma balloon flights).

[b] In early configuration (Texas balloon flights).

interval of best velocity resolution occurs for particles which have rigidities in the penumbra interval fo the Earth's magnetic field at our launch locations, a feature used in an analysis of isotopic abundances (Dwyer 1978; Dwyer and Meyer 1979). For relative elemental abundance measurements, this identifies the *lower* energy bound *above which no influence of the geomagnetic field is seen in the data*, i.e., above which the true unfiltered abundances can be measured. This is 1200 MeV n^{-1} for these flights. The *upper* energy limit for these measurements, 2400 MeV n^{-1}, is set in the data analysis. Below this energy the corrections for charge overlap of adjacent element distributions and the correction for the finite energy resolution of the Cerenkov counter are both zero; i.e., no corrections are necessary at all.

For a more complete description of the instrument the reader is referred to Dwyer, Jordan, and Meyer (1984). The balloon flight history of the two configurations of the experiment is given in Table 2. Note that the total exposure factor for the flights is 37.6 m^2sr hr.

III. DATA ANALYSIS

The data analysis procedures for the first two flights (Table 2) of the original instrument configuration were discussed in Dwyer (1978). Although data from all four flights have been reduced by very similar methods, where there are differences we here discuss the methods used in the latter two flights. Data for the largest part of the charge range for this paper comes from these latter two flights.

a) Corrections to the Raw Pulse Heights

Three corrections are applied to the raw pulse heights: (i) a correction for path length through the detectors consisting of multiplication by the cosine of the zenith angle of incidence; (ii) correction for nonuniformity of response of each detector, depending on where the particle passes through each detector; (iii) a correction for gain drift of the electronics. In each case the *residual* error after correction amounts to a few tenths of a percent.

b) Event Selection Criteria

The purpose of the event selection criteria is to eliminate background events and events in which a nucleus spallates in the matter of the instrument. It is important to do this in a way which does not introduce a systematic charge or energy-dependent bias. Nuclear interactions are eliminated by imposing consistency requirements on the various detector pulse heights since a fragmenting nucleus will show a lower pulse height after spallation. In an instrument with high charge resolution even the stripping of a single proton while traversing the instrument is detectable. Background is higher in the region of elements with low Z and is believed mainly to be due to the copious flux of cosmic-ray protons and helium interacting in the atmosphere above and around the instrument to produce a multiparticle event simulating a nucleus in the charge range considered. The strongest event selection criterion is therefore a straight-line trajectory within the MWPC hodoscope, unaccompanied by any second particle track.

The second selection criterion is that the ratio of the two scintillator pulse heights T1 and T3 agree within certain limits. These limits are T1/T3 = $\pm 9\%$ for oxygen and $\pm 5\%$ for iron. This helps to eliminate spallation reactions in the instrument. In order to impose this criterion so as not to introduce any charge or velocity-dependent bias we first verified that changes in the T1/T3 distributions within this energy range were negligible. They do change with Z, however, becoming narrower at higher Z. Since they are well fitted by Gaussians, they may be characterized by a single parameter, the standard deviation for each Z, $\sigma(Z)$. These are entered in our selection program so that multiple runs may easily be made seeing the effect of varying the parameter r, where the program accepts only events within $\pm r\sigma$ of the mean of T1/T3. Our results are insensitive to the choice of r over the range 1.5–3.0.

The third and last selection criterion, agreement of the instrument's two measures of charge, will be covered in the next subsection.

c) Charge Measurement

The goal of the data analysis is to use all the information available to form two functions of the pulse heights, one with the maximum charge resolution the other the maximum energy resolution.

If a matrix is accumulated by plotting one Cerenkov pulse height against another, events with the same nuclear charge Z will fall on a single straight-line track for energies above both thresholds. Figure 2 shows a matrix of such events from the balloon flights for the charge range $Z > 12$. Since the tracks are linear (strictly true only if ionization losses which change the velocity in the instrument are negligible), a rotation of the

TABLE 2

BALLOON FLIGHT SUMMARY

Flight Number	Launch Site (nominal cutoff vertical incidence)	Launch Date	Duration at Float (hr)	Mean Residual Atmosphere (g cm^{-2})	Exposure Factor (good data) (m^2sr hr)	Comments on Balloon Trajectory
1.....	Palestine, TX (4.5 GV)	1973 Sep 29	41	3.8	10.3	drifted to lower geomagnetic cutoff (3.4–4.6 GV)
2.....	Palestine, TX (4.5 GV)	1974 May 7	36	3.6	9.0	drifted to higher cutoff (4.3–5.8 GV)
3.....	Muskogee, OK (3.4 GV)	1975 Sep 23	44	4.7	10.5	range of cutoffs (3.0–4.2 GV)
4.....	Muskogee, OK (3.4 GV)	1975 Oct 1	33	3.6	7.8	nearly constant cutoff (~3.3 GV)

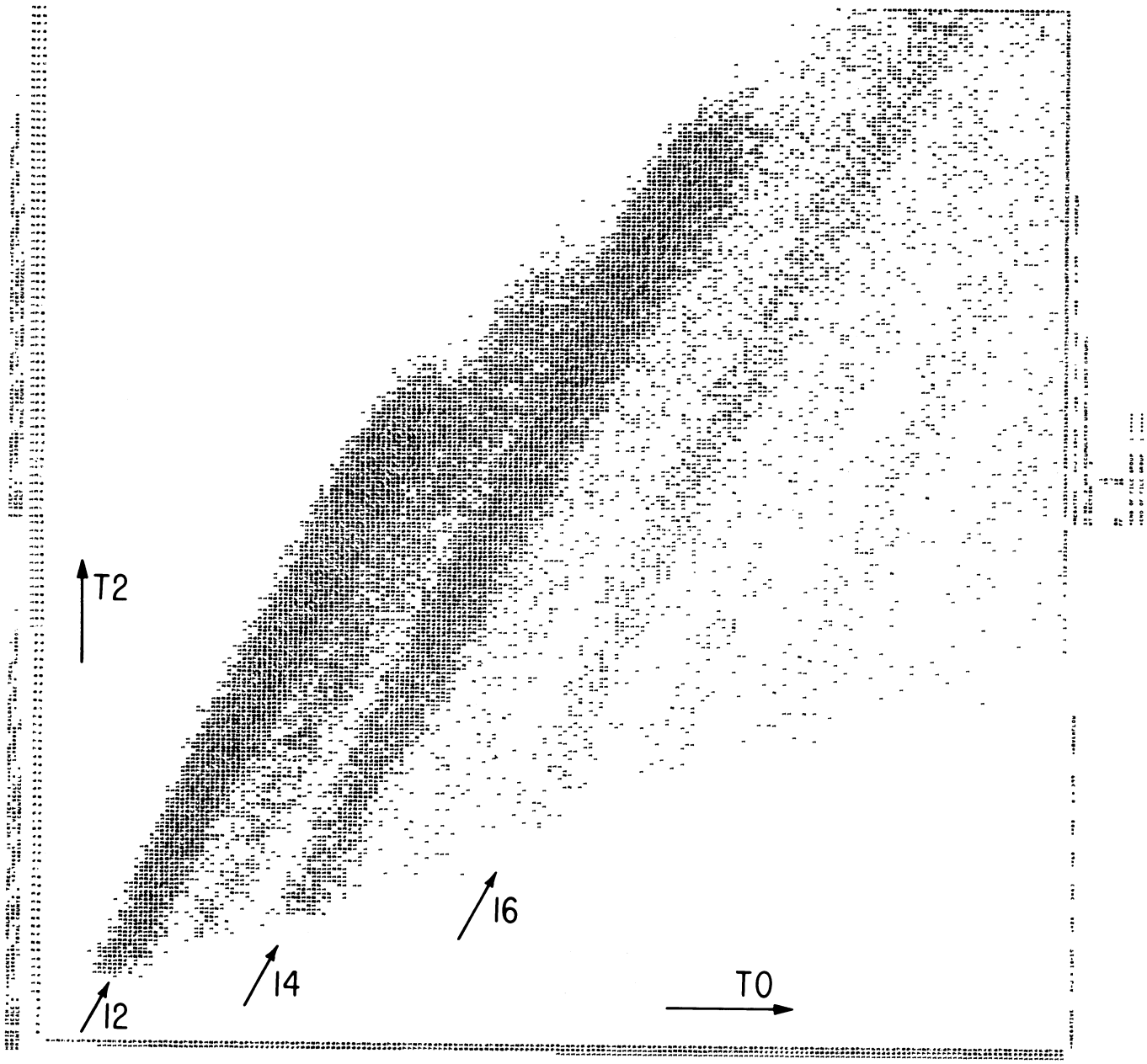

FIG. 2.—Matrix of the liquid Cerenkov counter pulse height T2 vs. the plastic Cerenkov counter pulse height T0 showing the tracks for the elements Mg, Si, and S ($Z = 12, 14, 16$).

matix will produce a representation where all the Z information is in one dimension (denoted CZ), and all the energy or velocity information is in the other dimension (denoted CV).

As discussed in Dwyer, Jordan, and Meyer (1984), the optimum charge resolution of the instrument is obtained from the function

$$U = 0.375(\mathrm{T1} + \mathrm{T3}) + 0.270\ \mathrm{CZ}\ . \qquad (1)$$

Since the Cerenkov response is proportional to Z^2, and, because of saturation, the scintillator response is not, these proportions are for $Z = 26$ At lower Z the scintillator portion of this function is increased.

A master matrix can now be formed of the function U versus CV chosen as the instrument's best measure of velocity. Individual charge tracks are separated on such a matrix over the whole range of Z. It was found, however, that if events from only one charge track (U versus CV matrix) were plotted in a (T1 + T3) versus CV matrix, "shadow" tracks of neighboring charges were seen, indicating the presence of nuclear interactions and a small residual background. Thus a very powerful selection criterion for noninteracting nuclei was that events be on the same charge track in both the U versus CV and the T1 + T3 versus CV matrix (this is also seen to be a consistency requirement between the two measures of Z, T1 + T3 and CZ). That is the final event selection criterion referred to in the previous subsection.

A matrix of U versus CV for the iron group is shown in Figure 3, showing the separation of the track for the rare

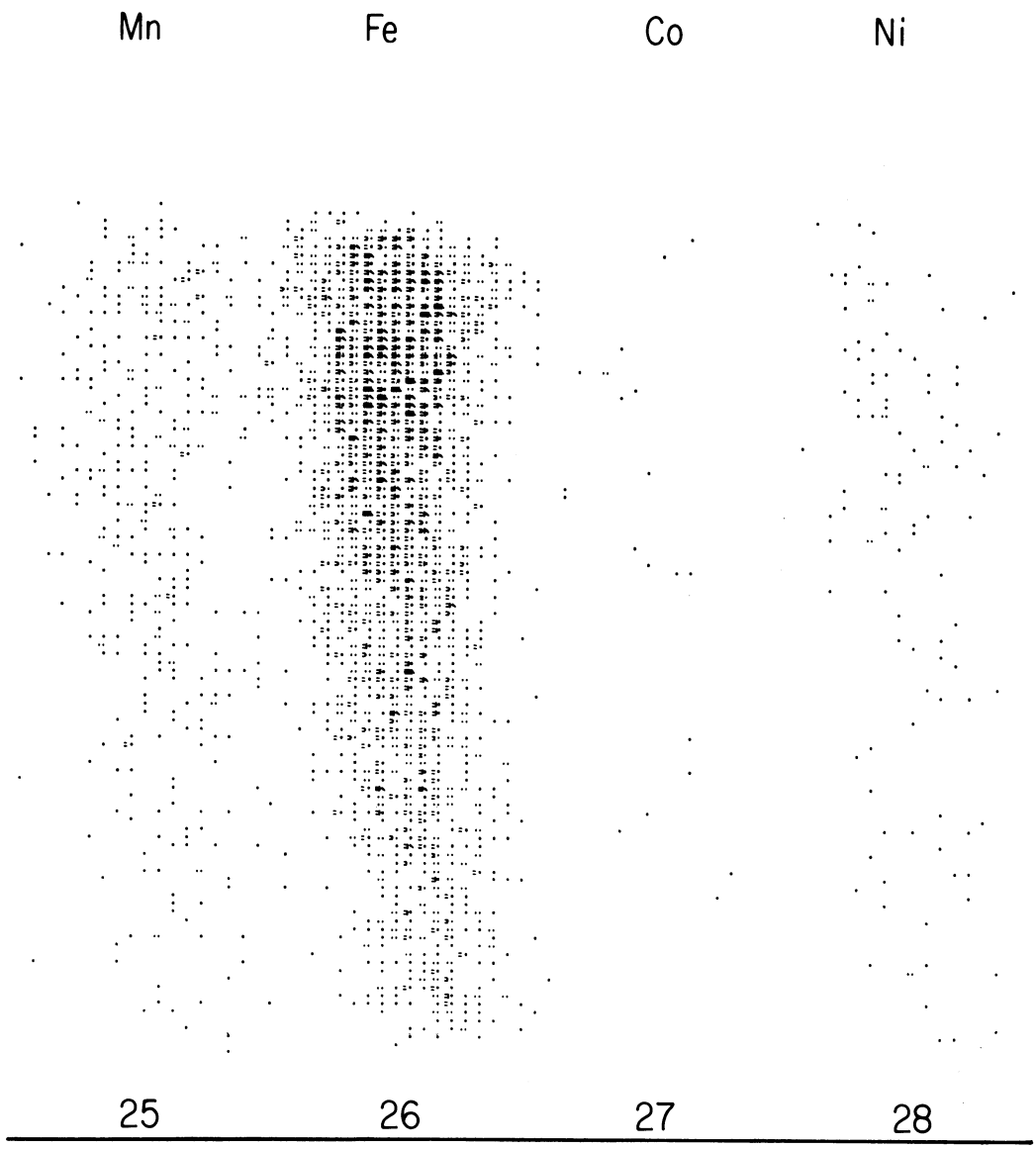

FIG. 3.—Matrix of energy (1.2–2.4 GeV n^{-1}) vs. charge for $Z = 25$–28

element cobalt from the neighboring iron track. For this energy range we find that no charge overlap corrections are necessary at all for these data. Thus we feel an important source of potential systematic errors is significantly reduced or eliminated. Figure 4 shows a charge histogram obtained by summing along these charge tracks after application of the selection criteria for the charge range $Z = 15$–28. Good charge separation is seen over this charge span. For lower Z ($Z = 5$–14) the resolution is comparable or better than shown here (Dwyer 1978). The charge resolution is 0.09 charge units at carbon, increasing to 0.20 charge units at iron.

d) Energy Measurement

The energy measurement requirements for this data set are minimal: define the lower and upper bound of one energy bin. As mentioned in § II, the lower bound of 1200 MeV n^{-1} eliminates all particles whose geomagnetic transmission is less than 100%. The upper bound of 2400 MeV n^{-1} is set to eliminate any need for charge overlap corrections and Cerenkov deconvolution corrections. In general, the energy or velocity resolution of a Cerenkov counter is very good just above the threshold decreasing to higher energies. For a given velocity, the resolution improves as Z increases because of increases in the amount of light emitted. In the case of the liquid Cerenkov counter T2, we found that above $\sim$2400 MeV n^{-1} the energy resolution of the counter was not sufficient to define this upper end of the energy bin for the lowest values of Z included without a correction being applied. This deconvolution of the measured signal spectrum to obtain the true energy spectrum is a regular feature of Cerenkov counter data analysis discussed in the literature (Juliusson 1974; Lezniak and Webber 1978). However, it is clear that taking a special subset of data where no such procedure is necessary at all will certainly help to reduce any systematic errors. Since corrections for energy resolution would be necessary to T0 in this energy range, we define our energy bin from the T2 signal alone.

To derive correctly the velocity of a particle from its pulse-height signal, a complete model of the sources of light emission

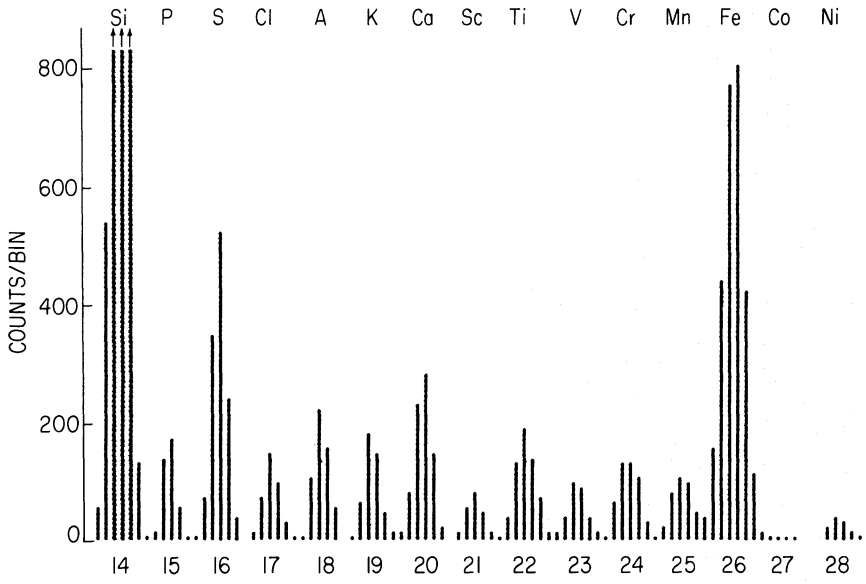

FIG. 4.—Charge histogram obtained in the balloon flights for the energy range 1.2–2.4 GeV n^{-1}

is required. For the liquid counter T2 the components included are given in Table 3. The energy dependence of these contributions is shown in Figure 5. Based on the calculations of Evenson (1975), we find the contribution from δ-rays to be best approximated by two components of Cerenkov light with differing indices of refraction. For details the reader is referred to Dwyer, Jordan, and Meyer (1984).

We have also developed a model for the fluctuations in the light emitted in T2, the liquid counter. Included are fluctuations in photoelectrons collected, the δ-ray light, and a third residual component which is a fixed percentage of the signal. The first two scale as $1/Z$, whereas the third is constant and independent of Z (1.3%). Figure 6 shows the signal dependence of these contributions for a given Z.

In connection with the energy measurement we now note how the correction for ionization loss in the atmosphere is done (the correction for nuclear spallation in the atmosphere is discussed in the next subsection). This correction is done on an event by event basis, using the actual amount of atmosphere traversed obtained from the pressure at that moment and the particle zenith angle of arrival. Since the specific ionization loss is not strongly energy dependent near its minimum at ~ 2 GeV n^{-1}, the dependence of the correction on the measurement of energy is minimal. Two independent pressure-measuring systems were used in all flights, with the results agreeing to within 0.1 g cm^{-2}. The measurements reported in this paper thus are for the energy interval 1200–2400 MeV n^{-1} after correction to the top of the atmosphere.

e) *Interaction Corrections*

Nuclear spallations occur in the matter of the instrument and in the overlaying atmosphere, and thus two corrections must be applied to get from the measured composition to the results at the top of the atmosphere. Interactions in the instrument are eliminated by the selection criteria, so a correction is necessary to derive the relative abundances at the top of the instrument. We calculate the total charge-changing interaction cross section using a geometrical model (Bradt and Peters 1950).

$$\sigma_{\Delta Z \geq 1} = \pi r_0^2 (A_{\rm CR}^{1/3} + A_T^{1/3} - b)^2 \, . \qquad (2)$$

Based on accelerator measurements at the Bevalac, Westfall *et al.* (1979) find a best fit with the parameters $\pi r_0^2 = 57.3$ mb and $b = 0.83$, and we have used their results. Although a significant fraction of the events undergo such a nuclear interaction (20% of C, almost 40% of Fe), the relative interaction correction

TABLE 3

MODEL FOR COMPONENTS OF THE LIGHT EMISSION IN T2 LIQUID CERENKOV COUNTER

Source	Description	Index of Refraction Assumed	Percent of Light Emitted at $\beta = 1$
1.....	Cerenkov light from primary	1.270	84.7
2.....	Cerenkov light from δ-rays:		
	Component A	1.270	5.5
	Component B	1.063	2.3
3.....	Cerenkov light from the mylar lid	1.60	1.4
4.....	Residual scintillation of the liquid or wavelength shifter	...	4.7
5.....	Cerenkov light in the $BaSO_4$ white paint	1.60	1.4

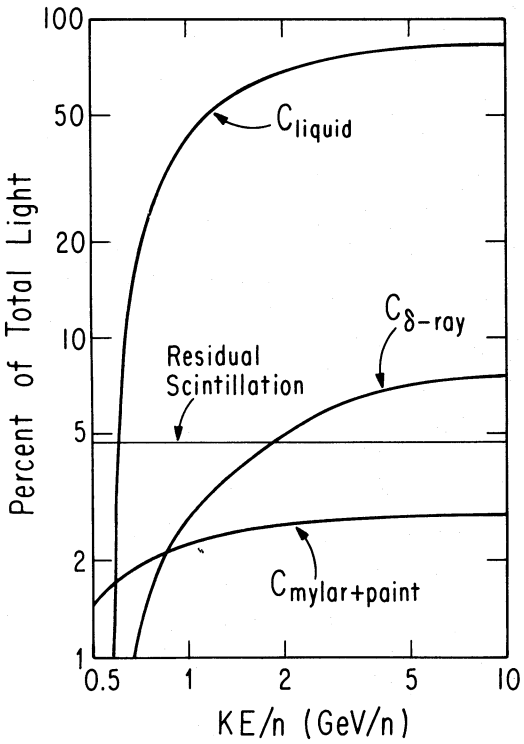

FIG. 5.—Components of the light emission in T2 liquid Cerenkov counter. The amount of Cerenkov light vs. kinetic energy per nucleon from the primary particle in the liquid, from δ-rays, and from the primary in the mylar and paint are shown along with the residual scintillation (assumed constant over this energy range).

TABLE 4

NUCLEAR INTERACTION CORRECTIONS

Z	Instrument	Atmosphere
5.....	0.886	0.776
6.....	0.897	0.898
7.....	0.913	0.830
8.....	0.925	0.945
9.....	0.945	0.756
10.....	0.954	0.913
11.....	0.969	0.808
12.....	0.978	0.963
13.....	0.993	0.878
14.....	1.000	1.000
15.....	1.016	0.869
16.....	1.025	0.980
17.....	1.042	0.855
18.....	1.050	0.990
19.....	1.065	0.797
20.....	1.074	0.934
21.....	1.092	0.823
22.....	1.103	0.882
23.....	1.116	0.839
24.....	1.126	0.966
25.....	1.137	0.918
26.....	1.148	1.136
27.....	1.163	0.945
28.....	1.162	1.161

varies over a much narrower range. The interaction corrections we have used are given in Table 4. We have also checked that if the interaction cross sections have 20% errors in them, this contributes less than a 3% error in the relative abundances.

Since the composition is altered by production and loss of particles via nuclear interactions in the atmosphere, a correction has been applied to the data for this effect also. Over the course of our balloon flights there was remarkably little variation in float altitude, and our data sample is based on a depth range of 3.0–4.5 g cm^{-2} (average = 3.7 g cm^{-2}). Taking into account the mean angle of incidence over our telescope's opening angle ($\theta = 21°$) and the amount of matter in our instrument above the top detector (considered part of the atmospheric correction), we arrive at 6.2 g cm^2 for the amount of atmosphere to be corrected for.

We use a model which propagates the cosmic rays through a slab of uniform thickness and which has as the major input the nucleus-nucleus fragmentation cross sections. The partial frag-

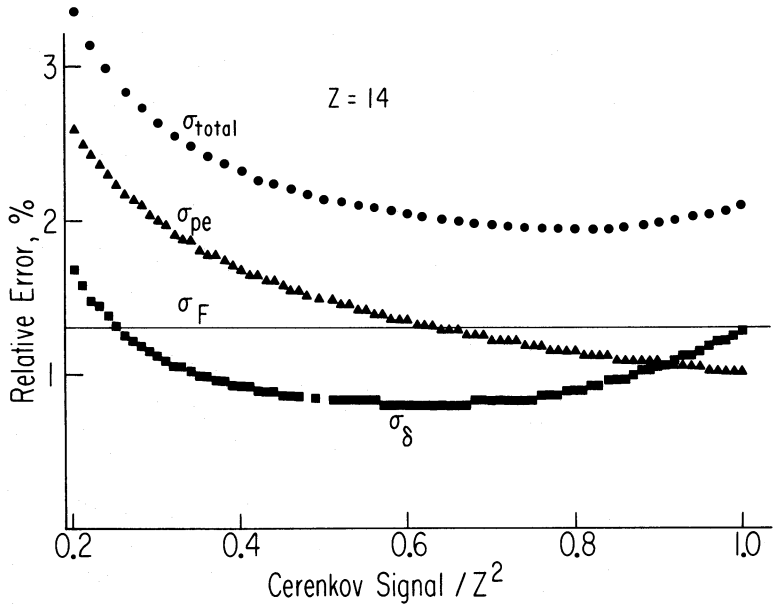

FIG. 6.—Relative standard deviation (σ/mean) in percent from various sources of signal fluctuations in the T2 liquid Cerenkov counter. The contributions from photoelectron fluctuations, σ_{pe}, fluctuations in light from δ-rays, σ_δ, and a residual component which is a "fixed" percentage of the signal are shown.

mentation cross sections are based on the semiempirical results of Silberberg and Tsao (1973*a*, *b*). The total reaction cross sections are from Meyer, Cassé, and Westergaard (1975) and differ only negligibly from those of Westfall *et al.* (1979). This calculation includes 226 nuclides up to ^{64}Ni with half-lives for decay greater than 10^{-6} s. The resulting abundances versus depth were summed over the isotopes to give the flux for each element.

However, all these cross ections are not well known, and a preferable method would be to use abundances measured as a function of atmospheric depth to derive the absorption length of each cosmic-ray element. Our flights did not sample a wide enough range of depths to give accurate results for this method, but Israel *et al.* (1979) have reported results of such an analysis with good statistical accuracy which provide empirical atmosphere attenuation curves for all elements with $13 \leq Z \leq 28$. The variation of the relative abundances with depth was well fitted by exponentials. We have used their results to generate atmospheric correction factors for $Z > 13$ and the semiempirical slab model calculation for the lower charges. The atmospheric corrections are given in Table 4. We note that there is less uncertainty in these relative corrections than would be if absolute fluxes were measured.

IV. RESULTS

The results of the data analysis discussed in the previous section are the relative abundances at the top of the atmosphere for boron through nickel ($Z = 5$–28) at 1200–2400 MeV n^{-1}. These are given in Table 5, normalized to Si. For oxygen and heavier elements ($Z \geq 8$), the errors quoted are statistical. As mentioned in § II, these data are derived from our flights from Oklahoma (Table 2). The boron through nitrogen data are derived from our flights from Texas, and a 3% error has been included to account for normalization uncertainties.

TABLE 5

RELATIVE ELEMENTAL ABUNDANCES

Element	Z	Abundance
B	5	1920 ± 143
C	6	6400 ± 211
N	7	1820 ± 58
O	8	5930 ± 107
F	9	143 ± 7.4
Ne	10	993 ± 26
Na	11	224 ± 8
Mg	12	1240 ± 28
Al	13	224 ± 8
Si	14	1000
P	15	51.1 ± 3.5
S	16	189 ± 8
Cl	17	47.1 ± 3.4
Ar	18	79.5 ± 4.9
K	19	57.0 ± 3.7
Ca	20	124.4 ± 6.3
Sc	21	28.5 ± 2.6
Ti	22	82.1 ± 4.8
V	23	41.0 ± 3.3
Cr	24	80.9 ± 5.0
Mn	25	59.9 ± 4.1
Fe	26	587 ± 17
Co	27	4.1 ± 1.1
Ni	28	24.0 ± 2.9

NOTE.—At the top of the atmosphere, normalized to Si.

In Figure 7 the results are compared with other recent measurements in which the normalization is to Si = 1000. In the case where other experimenters cover a wide energy range, the data most closely overlapping our energy interval were selected. This energy interval is noted in the symbol key to the figure. Only the work by Garcia-Munoz and Simpson (1979) which is based on satellite results is at much lower energy. Thus, with the exception of this case, any dependece on energy is eliminated by comparing data measured over essentially the same energy interval.

We note generally good agreement among the various experiments in this energy range. In particular, the two experiments that cover the entire charge range at GeV n^{-1} energies, ours and the *HEAO* C experiment (Engelmann *et al.* 1983), show very good agreement. These two experiments have both high statistical accuracy resulting from long exposures and unambiguous charge resolution to separate each element distribution over the charge range considered here. An exception is the element Ni where Engelmann *et al.* find an abundance somewhat higher than ours. When the Ni/Fe ratios are compared instead of normalizing to Si there is no significant discrepancy, indicating the possible presence of a small Z-dependent systematic effect which only appears when comparing ratios of elements widely separated in Z.

This is seen more clearly in Figure 8 where just the charge range $Z = 15$–28 is examined, normalized to Fe, and plotted on a linear vertical scale. Many of the same data are compared in this figure, except for those of Lezniak and Webber (1978) where integral data above 450 MeV n^{-1} are included. In Figure 8 the striking agreement between our experiment and that of Engelmann *et al.* (1983) is clearly seen over this charge range. The statistical accuracy of the *HEAO* C experiment is considerably better than all previous experiments. Over this important energy range, agreement between the two experiments with the highest statistical precision and the best charge separation provides confidence that the element abundances are known to within a few percent.

We also note that in the case of some of the underabundant odd-Z elements improved charge resolution leads to lower abundances by elimination of uncorrected spillover from neighboring more abundant elements. In particular, for F, P, Sc, V, and Mn both this experiment and that of Engelmann *et al.* (1983) observe lower abundances than previously measured (Figs. 7 and 8).

V. DISCUSSION AND CONCLUSION

a) Implications for Cosmic-Ray Propagation

The results obtained and presented in the last section may now be used to obtain implications for models of cosmic-ray propagation and confinement in the Galaxy. The simplest propagation model is one in which the Galaxy is pictured as a large containment volume with a small but finite probability for the particles to escape at the boundary—the so-called "leaky-box" model. The propagation is then characterized by a single number, the mean of the path length distribution (exponential in shape for this model). It is well known that this mean path length decreases with increasing energy above a few GeV n^{-1}. Recent results point to a decrease of this mean with decreasing energy at $\sim$100 MeV n^{-1} also (Garcia-Munoz *et al.* 1979). Thus a measurement of the mean path length at 1–2 GeV n^{-1} is very valuable since this energy range is below

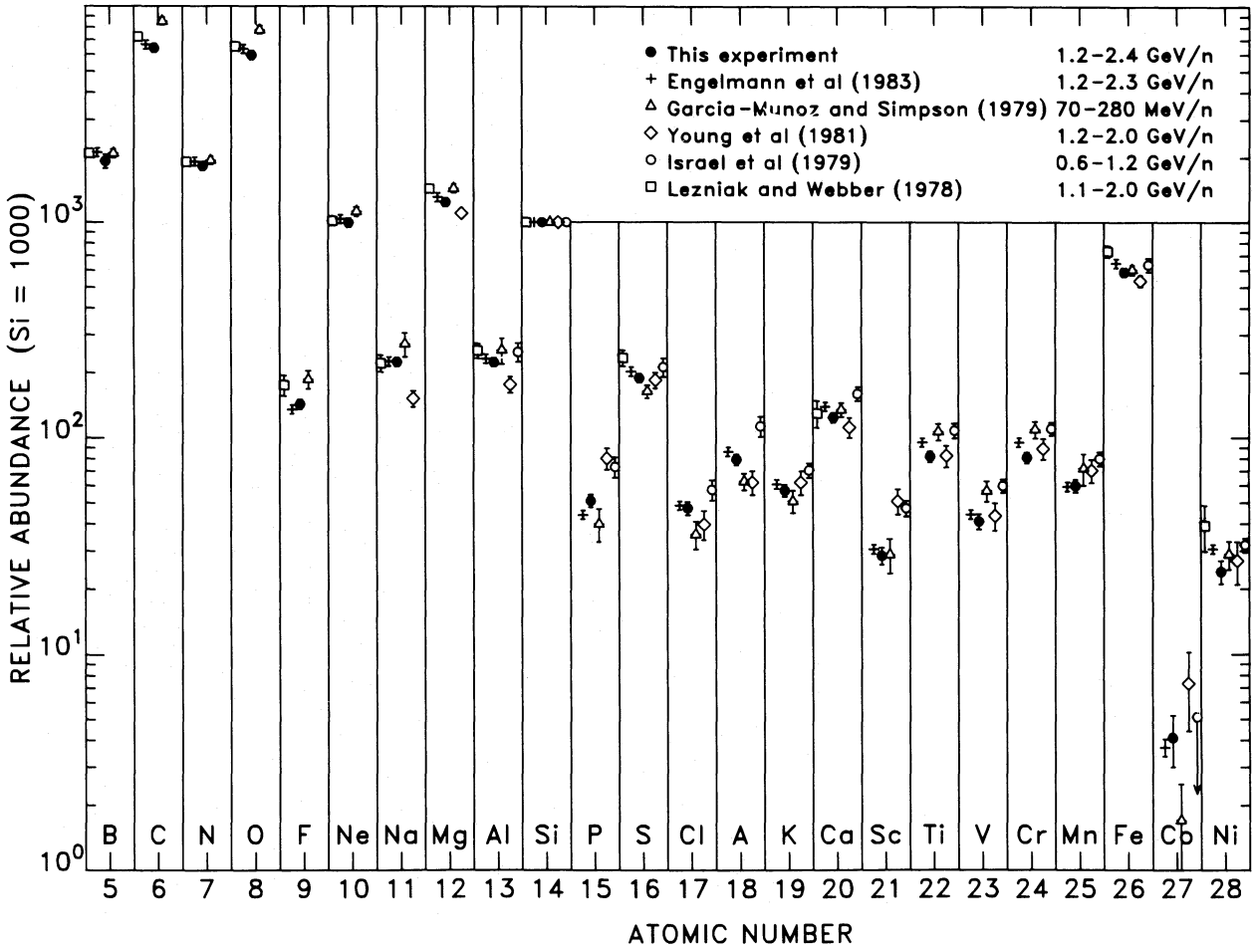

FIG. 7.—Relative elemental abundances as measured at the top of the atmosphere by several investigators

that where the falloff to higher energy occurs and above the range where the low-energy decrease is thought to occur.

In addition, the measurements at lower energy are complicated by the need to unfold the large effects of solar modulation which, at our energies, play a relatively small role. We note the importance of nuclear spallation cross sections in the calculation of the effects of interstellar propagation. Many of the measurements of cross sections have been done at an energy of ~ 1 GeV n^{-1}, directly applicable to results of this experiment and requiring no assumption on the shape of the excitation function versus energy. Finally, interstellar ionization loss, although an effect which definitely should be included in propagation calculations, is of lesser importance at our energies.

We have done extensive propagation calculations using a model which we will now describe. The interstellar medium composition is assumed to have a helium to hydrogen ratio of 0.067 (Cameron 1982). Assuming pure hydrogen results in a $\sim 20\%$ decrease in the mean path length required to match the measured abundances. The mean interstellar density is 0.4 atoms cm^{-3}, which corresponds to an average confinement time in the Galaxy of $\sim 1.1 \times 10^7$ yr at this energy. Variation of this parameter only affects radioactive nuclei and their decay products. Our calculation takes into account decays of ^{10}Be, ^{26}Al, ^{36}Cl, ^{54}Mn, and ^{60}Fe. The total reaction cross section of the cosmic rays on the interstellar material is given by the high-energy formula of Letaw (1983). His Table 2 shows that this formula reproduces experimental results more closely than the work of Tsao and Silberberg (1975), Hagen (1976), and, according to our calculation, Westfall *et al.* (1979). The partial cross sections are calculated according to Silberberg and Tsao (1973*a*, *b*) with updates (Silberberg and Tsao 1977; Tsao and Silberberg 1979). The source spectral shape is chosen to be $(T + 400)^{-2.4}$, although variation of the spectral index by ± 0.2 results in negligible change in the results for this energy interval. Solar modulation using the force-field model of Gleeson and Axford (1968) is taken into account, with $\phi = 250$ MeV n^{-1} for the interplanetary deceleration parameter, for nuclei with $A/Z = 2.0$.

We conclude that a pure exponential path length distribution is the best fit to our data. We assume zero source abundance for the elements B, F, Sc, and V($Z = 5, 9, 21, 23$) and find that this path length distribution fits all our measured abundances for $Z = 5$–28 at an energy of 1.2–2.4 GeV n^{-1}. The escape mean free path we obtain is

$$\lambda_e = (7.6 \pm 0.8) \text{ g cm}^{-2} ,$$

where the error is based on the measurement error only. The only exception is Ti ($Z = 22$) where a negative source abundance would be required to match the data. It is possible that the semiempirical cross sections have been overestimated for this element as noted previously (Dwyer *et al.* 1981; Perron

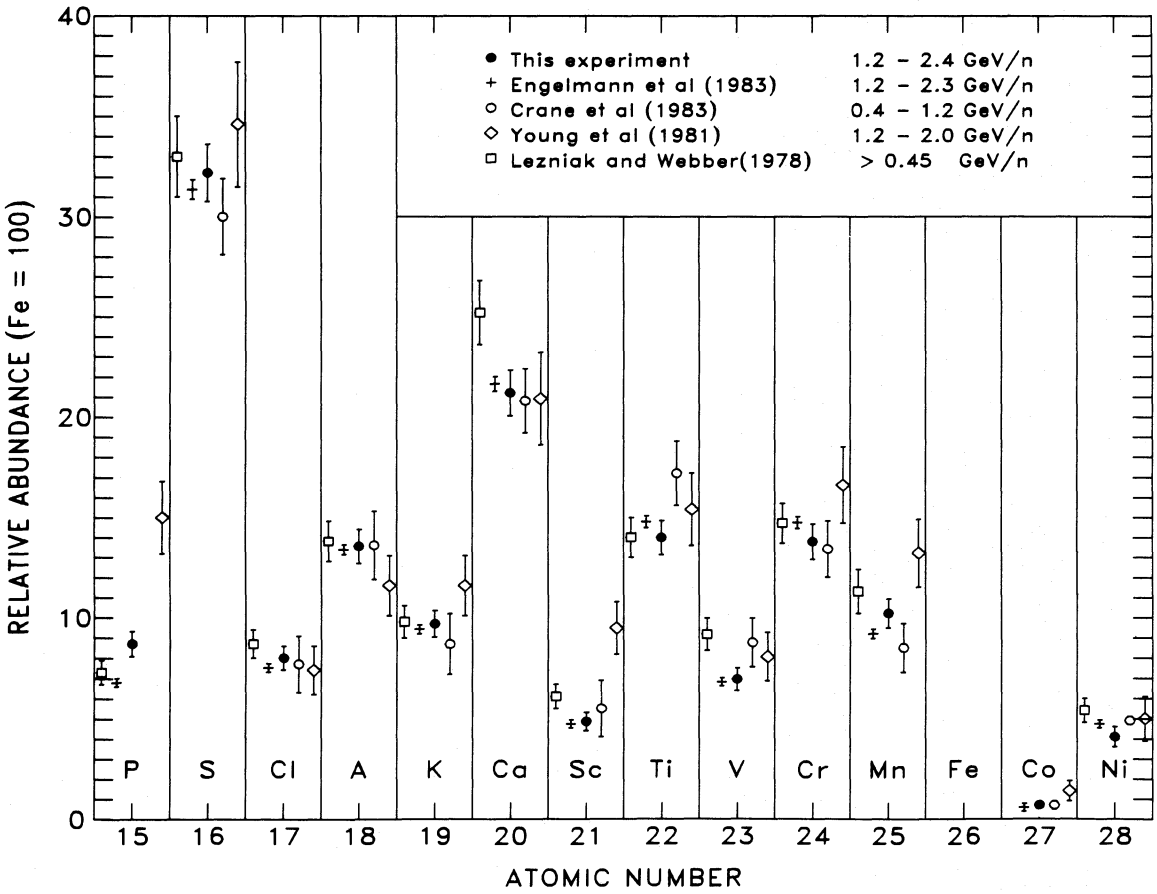

FIG. 8.—Relative elemental abundances normalized to Fe = 100 on a linear scale

and Koch 1981) and indicated in recent results of Webber (1985).

Our data do not require a truncated exponential path length distribution as might be expected from some models, e.g., a nested leaky-box model. However, we cannot exclude a small amount of truncation (<0.5 g cm^{-2}). This is in agreement with the analysis of Protheroe, Ormes, and Comstock (1981) and Ormes and Protheroe (1983), who concluded that 8% of the matter traversed could be in the source regions. The mean path length that we deduce is in good agreement with the most recent results of the *HEAO* C-2 experiment (Lund 1985) which, for particles with rigidities below 5.5 GV yields a mean escape length of (7.9 ± 0.7)g cm^{-2}. At lower energies ($\sim$100–300 MeV n^{-1}), Garcia-Munoz and Simpson noted that a pure exponential path length distribution fails to reproduce both the subiron/iron and the B/C ratios using their data from the *IMP 8* satellite. They find an energy-dependent truncation of short path lengths is necessary, where the amount of truncation decreases with increasing energy. The truncation predicted above 1 GeV n^{-1} is less than 0.5 g cm^{-2}, in agreement with our results.

b) Cosmic-Ray Source Abundances

The results of the calculation in the previous subsection are used to arrive at the cosmic-ray source abundances. These are given in Table 6, normalized to Si = 1000 at an average energy of $\sim$2 GeV n^{-1}.

Errors in the derived source abundances arise both from errors in the abundances measured at Earth and from uncertainties in the propagation calculation, e.g., cross sections and parameters in the model. The relative contributions are different for different elements. To evaluate the contribution of errors from the propagation calculation we have relied on the calculation of Hinshaw and Wiedenbeck (1983). Their results are for the 820–1290 MeV n^{-1} data from the *HEAO* C-2 experiment reported in Engelmann *et al.* (1983) which should

TABLE 6

ABUNDANCES AT COSMIC-RAY SOURCE

Element	Relative Abundance
C	4130 ± 346
N	490 ± 303
O	4720 ± 248
Ne	608 ± 75
Na	86 ± 38
Mg	1051 ± 69
Al	124 ± 36
Si	1000[a]
P	22.6 ± 10
S	122 ± 20
Ca	41 ± 29
Fe	833 ± 50
Co	4.3 ± 2.0
Ni	37 ± 8

[a] Normalization.

apply to our data as well. Specifically, contributions were evaluated for an assumed error in the total reaction cross section of $\pm 5\%$ and in the mean escape length of ± 0.5 g cm^{-2}. For the partial cross sections, results for two extremes are presented: one in which the errors in the partial cross sections are uncorrelated, and the other in which they are completely correlated. We have used the average of these two cases as an estimate of this rather uncertain contribution to source abundance errors. Since a large uncertainty of $\pm 35\%$ was assumed in their work, this should represent a conservative approach to this part of the error. The reported errors in our source abundances given in Table 6 are then the result of combining our observational error with these errors from the propagation calculation. It should be noted that the propagation error strongly dominates the measurement error for N and Ca ($Z = 7, 20$). For Cr and Mn ($Z = 24, 25$), a finite flux at the source would be obtained if only the measurement error were included. However, this is no longer possible if the propagation error is taken into account.

Figure 9 compares these results with other recent calculations of the cosmic-ray source abundances. The results of Koch-Miramond *et al.* (1983) and Perron *et al.* (1981) are both from the data of the Danish-French experiment aboard the *HEAO* 3 satellite. This provides an idea about the degree of uncertainty introduced in the extrapolation to the source. The errors in the results presented in Figure 9 cannot be directly compared because not all investigators evaluate the contribution from the propagation error in the same manner. In the calculation of Adams *et al.* (1981) no errors were reported, so none are included here. All of these results are for an energy of ≥ 1 GeV n^{-1}.

In our results we see a definite indication of a source component for phosphorus ($Z = 15$) which is not seen in some of the other work. Since our measurement for phosphorus (Figs. 7, 8) is somewhat higher than that of Engelmann *et al.* (1983), this may partially explain the difference. On the other hand, our results do not require a finite source abundance for argon ($Z = 18$) which is seen by others. Note that in Figure 8 our measurements for Ar agree very well with Engelmann *et al.* (1983), so this discrepancy must be in the propagation calculation. However, an upper limit from our measurement, including the propagation error, would not be substantially below the data points for argon in Figure 9. This case is influenced by the contribution from ^{36}Cl decay which must be taken into account properly. We also note reasonable agreement between our source abundances and those of Young *et al.* (1981) for S, Ca, Fe, and Ni.

It is of interest to compare these abundances in the cosmic-ray source with the so-called universal or solar system abundances (Cameron 1982). This is done in Figure 10 where the ratio of abundances in the source over abundances in the solar system normalized at Si is plotted versus first ionization potential, a frequently used parameter thought to bring some order to the data. As is well known, elements like S, C, N, O, and Ne are underabundant in the cosmic-ray source relative to the solar system. These are just the elements with higher first ionization potential. Although it is clear that the first ionization potential (FIP) does provide some ordering of the data, the

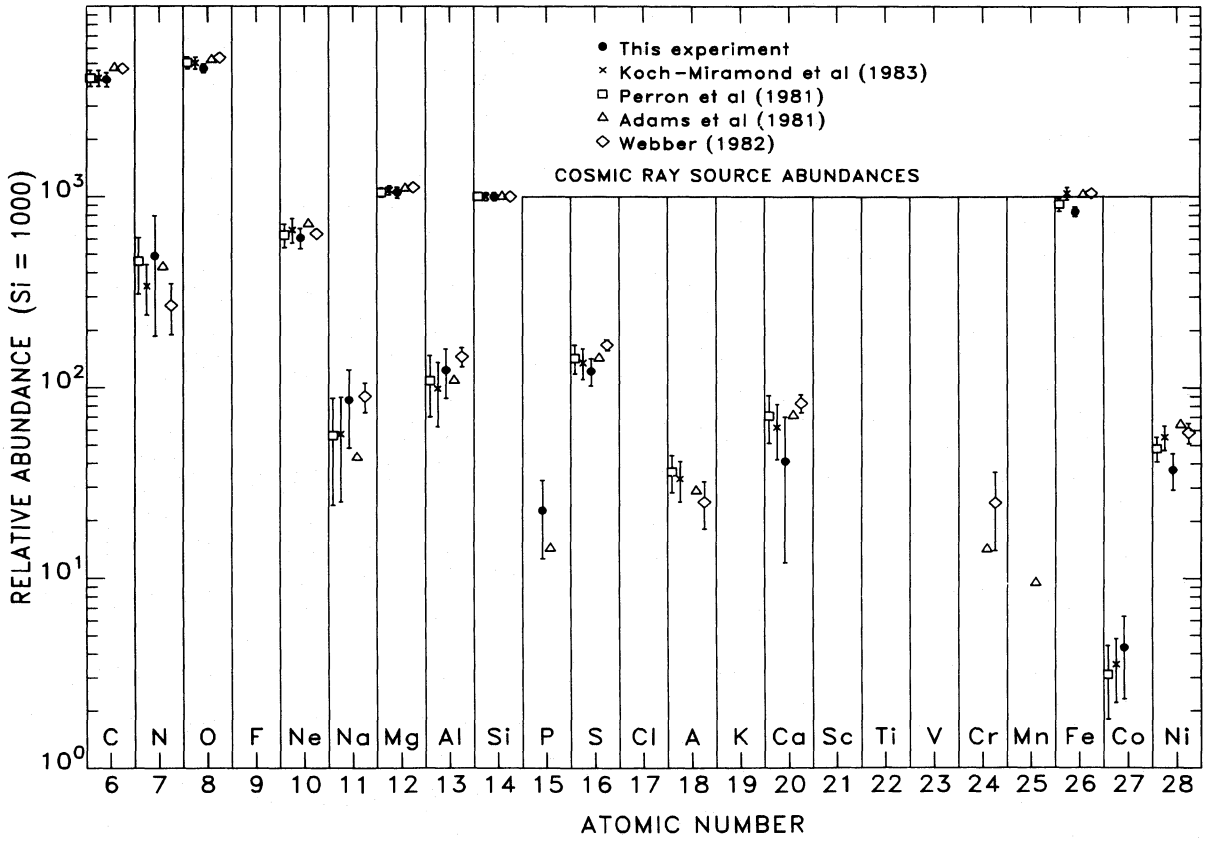

FIG. 9.—Cosmic-ray elemental source abundances at 1–2 GeV n^{-1}

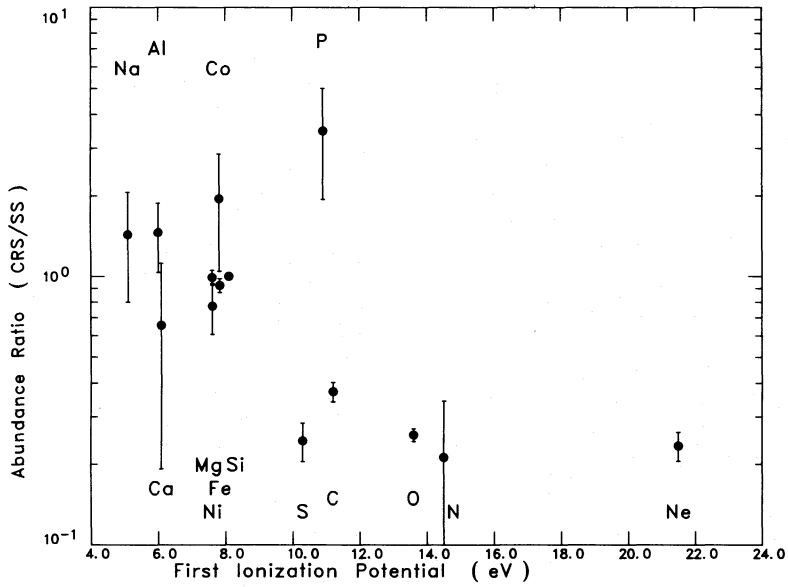

FIG. 10.—Cosmic-ray source to solar system abundance ratio vs. first ionization potential

specific form of this dependence is not yet clear. It may be interpreted as a threshold effect, i.e., dividing the data into two groups, one with FIP $\leq$8–10 eV having a ratio $\sim$1, and another group with FIP $>$10 eV having a much lower value for the ratio. Alternatively, the dependence may be exponential, i.e., a linear decrease on the semilogarithmic plot (Fig. 10). However, in either case phosphorus stands out as an exception. Although the first ionization potential does provide a useful parametrization of the data, there are still well-known anomalies. We would include phosphorus in particular as a new anomaly.

c) Time Delay between Nucleosynthesis and Acceleration

The measured relative abundance of cobalt ($Z = 27$) can be used as an indicator of δt = the time delay between *e*-process nucleosynthesis and acceleration of cosmic-ray material (Soutoul, Cassé, and Juliusson 1978). As these authors point out, three cases may be distinguished depending on the value of δt.

Case 1: $\delta t \leq \sim 1$ yr. This time interval is too short to allow ^{57}Co (produced in the *e*-process as ^{57}Ni) to K-capture decay; thus, it is stable in the cosmic rays. We have redone the propagation calculation relevant to this problem and find that for case 1 an abundance Co/(Fe + Ni) = 2.4% is predicted at 1AU (Table 7). This is in agreement with the calculations of Soutoul, Cassé, and Juliusson (1978).

Case 2: 1 yr $< \delta t \leq 10^5$ yr. This intermediate delay is enough so that ^{57}Co decays in the source (which in the *e*-process calculations of Hainebach, Clayton, and Arnett 1974 yields the universal abundance of ^{57}Fe). However ^{59}Ni does not have time to K-capture decay and thus is stable in the cosmic rays. For this delay, there is no source cobalt, and all measured cobalt at Earth is of spallation origin. Our calculation predicts a ratio Co/(Fe + Ni) = 0.2% at 1 AU.

Case 3: $\delta t > 10^5$ yr. For very long time delays, the *e*-process nucleosynthesis yields solar system abundances after all decays have occurred. Thus cobalt at the source is all ^{59}Co, and the arriving cosmic rays have a predicted abundance Co/(Fe + Ni) = 0.7% at 1 AU.

With our experiment we measure the Co/(Fe + Ni) ratio to be (0.67 $\pm$ 0.18)% (Table 5). Conservatively, even if one-quarter of the cobalt events are considered misidentified as a measure of systematic errors, the result becomes (0.67 $\pm$ 0.25)%. Within the context of this model this result seems to favor the longest time delay $\delta t > 10^5$ yr.

However, note that the problem of distinguishing case 3 (longest delay) from case 2 (intermediate delay) reduces to determining a finite source abundance of cobalt. If only an upper limit can be derived, then the two cases cannot be distinguished. We derive a finite flux of cobalt at the source at the 2.1 σ level (Fig. 9) based on measurement error only. We believe that the errors in the propagation which are difficult to estimate (uncertainties in cross sections, model parameters, etc.) are large enough so that both case 2 and case 3 may be allowed conclusions based on our data.

A similar analysis of the data from the *HEAO* C-2 experiment was carried out Koch-Miramond (1981), who concluded that cases 1 and 2 were inconsistent with their data, i.e., that the time delay was "most probably" greater than 10^5 yr. The statistical accuracy of their data set is better than ours, and the charge separation is about equal in the two experiments for the rare element cobalt. We measure nearly identical abundances of cobalt at Earth (Figs. 7 and 8) and at the source (Fig. 9). We

TABLE 7

CALCULATION OF Co/(Fe + Ni) RATIO IN COSMIC RAYS FOR 1 AU

Model	Case 1 $\delta t \leq 1$ yr	Case 2 $1 \leq \delta t \leq 10^5$ yr	Case 3 $\delta t \geq 10^5$ yr
1 ..... Solar system source	2.4%	0.2%	0.7%
2 ..... Source neutron enriched	2.0%	0.2%	0.6%

NOTE.—In model 1 the isotopic composition at the source is taken from Cameron 1982. In model 2 the neutron-rich nuclei ^{60,61,62,64}Ni and ^{57,58}Fe are enhanced at the source by a factor 1.7 times solar system. In both cases source elemental composition is that which reproduces our measured relative abundances at 1 AU.

conclude case 3 is somewhat favored, but until the propagation contribution to the errors is better known, this result (case 3) cannot be considered firmly established. However, case 1 is ruled out by our analysis.

These results are based on a very specific model of nucleosynthesis developed by Hainebach, Clayton, and Arnett (1974). The abundances of iron group elements resulting from the nucleosynthesis occurring in the explosion of a massive highly evolved star are calculated for rapid cooling of material in nuclear statistical equilibrium at a temperature of more than 5 billion degrees ("*e*-process freeze-out"). In this case almost all the free, light nuclei (p, n, α) are captured, and the freeze-out occurs in a "particle-poor" fashion. Under these circumstances the final abundances depend basically on only one parameter, the neutron excess of the matter. The abundant isotopes in the iron-nickel group then are synthesized as their proton-rich progenitors; in particular, ^{56}Fe is made as ^{56}Ni. However, it is by no means obvious that a "particle-rich" freeze-out may not occur in nature (or any intermediate case either). The model of Hainebach, Clayton, and Arnett is the best current description of iron group synthesis which affects the initial source composition for the cosmic-ray problem. If new work should cause this picture to change, it may affect the composition which ultimately produces agreement with the solar system abundances.

It is further assumed that the initial cosmic-ray source isotopic composition (which is then propagated to Earth to get the abundance distribution of arriving particles) is chosen so that it gives the universal abundances of Cameron (1982) after radioactive decays are allowed.

Observations in satellite experiments with good mass resolution at lower energies have shown enhancements of neutron-rich isotopes of elements like Ne, in particular, and, to a lesser extent, Mg and Si (see the recent review of Wiedenbeck 1985) in the cosmic-ray sources over solar system abundances. It is of interest to investigate whether the cobalt abundance would still be a useful time delay indicator if enhancements of neutron-rich isotopes were also observed for the iron group. To this end we have repeated the propagation calculation for the three cases, with a source isotopic composition enhanced in the neutron-rich isotopes for Fe and Ni. We used an enhancement factor (cosmic-ray source/solar system) of 1.7 which we derived as the best overall estimate of the average enhancements observed for the Ne, Mg, Si nuclei (Wiedenbeck 1985). The results are given under model 2 in Table 7. Although they differ slightly from those with solar system isotopic composition, they essentially show that the basic pattern remains unchanged for the three cases.

Only if highly pathological source isotopic compositions were considered would the conclusions be altered. Available results on the Fe isotopic composition show, however, that the predominant Fe isotope is ^{56}Fe, as expected (Mewaldt *et al.* 1980; Young *et al.* 1981; Tarlé, Ahlen, and Cartwright 1979; Webber 1981). We take this as strengthening the validity of the time-delay analysis which does not strictly depend on the assumption of solar system source ratios.

VI. SUMMARY

This paper presents a measurement of the relative abundances of cosmic-ray nuclei from boron through nickel ($Z = 5$–28) over the energy range 1200–2400 MeV n^{-1}. A pure exponential path length distribution in a simple leaky-box model of the Galaxy gives the best fit to the data. A small amount of truncation ($\lesssim 0.5$ g cm^{-2}) as in a nested leaky-box model cannot be ruled out, however. Values for the source abundances consistent with these measurements are given. Analysis of the Co abundance places the time delay between nucleosynthesis and acceleration at greater than $\sim 10^2$ days. The case for this delay being greater than 10^5 yr is indicated but not unequivocally established by these data.

We are greatly indebted to the technical staff of the Laboratory for Astrophysics and Space Research in the Enrico Fermi Institute, in particular, G. Kelderhouse, W. Johnson, W. Hollis, and L. Glennie. We wish to thank Dr. M. Wiedenbeck for the use of his computer code for propagation calculations and for helpful discussions. Also we thank Dr. G. Minagawa for preparation and execution of the Oklahoma balloon flights. The staff of the National Scientific Balloon Facility ably performed launch and recovery.

REFERENCES

Adams, J. H., Shapiro, M. M., Silberberg, R., and Tsao, C. H. 1981, *Proc. 17th Internat. Cosmic-Ray Conf.* (Paris), **2**, 256.
Bennegas, J. C., Israel, M. H., and Klarmann, J. 1975, *Proc. 14th Internat. Cosmic-Ray Conf.* (Munich), **9**, 3172.
Bradt, H. C., and Peters, B. 1948, *Phys. Rev.*, **74**, 1828.
———. 1950, *Phys. Rev.*, **77**, 54.
Cameron, A. G. W. 1982, in *Essays in Nuclear Astrophysics*, ed. by C. A. Barnes, D. D. Clayton, and D. N. Schramm (Cambridge: Cambridge University Press), p. 23.
Crane, J. H., Israel, M. H., Klarmann, J., Ormes, J. F., and Protheroe, R. J. 1983, *Ap. Space Sci.*, **94**, 211.
Dwyer, R. 1978, *Ap. J.*, **224**, 691.
Dwyer, R., Garcia-Munoz, M., Guzik, T. G., Meyer, P., Simpson, J., and Wefel, J. 1981, *Proc. 17th Internat. Cosmic-Ray Conf.* (Paris), **9**, 222.
Dwyer, R., Jordan, S., and Meyer, P. 1984, *Nucl. Instr. Meth.*, **224**, 247.
Dwyer, R., and Meyer, P. 1979, *Proc. 16th Internat. Cosmic-Ray Conf.* (Kyoto), **12**, 97.
———. 1981, *Proc. 17th Internat. Cosmic-Ray Conf.* (Paris), **2**, 54.
Engelmann, J. J., *et al.* 1983, *Proc. 18th Internat. Cosmic-Ray Conf.* (Bangalore), **2**, 17.
Evenson, P. 1975, *Proc. 14th Internat. Cosmic-Ray Conf.* (Munich), **9**, 3177.
Freier, P. S., Lofgren, E. J., Ney, E. P., Oppenheimer, F., Bradt, H. C., and Peters, B. 1948, *Phys. Rev.*, **74**, 213.
Garcia-Munoz, M., Margolis, S. H., Simpson, J. A., and Wefel, J. P. 1979, *Proc. 16th Internat. Cosmic-Ray Conf.* (Kyoto), **1**, 310.
Garcia-Munoz, M., and Simpson, J. A. 1979, *Proc. 16th Internat. Cosmic-Ray Conf.* (Kyoto), **1**, 270.
Gleeson, L. J., and Axford, W. I. 1968, *Ap. J.*, **154**, 1011.
Hagen, F. A. 1976, Ph.D. thesis, University of Maryland.
Hainebach, K. L. Clayton, D. D., and Arnett, W. D. 1974, *Ap. J.*, **193**, 157.
Heckman, H. H., Greiner, D. E., Lindstrom, P. J., and Bieser, F. S. 1972, *Phys. Rev. Letters*, **28**, 926.
Hinshaw, G. F., and Wiedenbeck, M. E. 1983, *Proc. 18th Internat. Cosmic-Ray Conf.* (Bangalore), **9**, 263.
Israel, M. H., Klarmann, J., Love, P. L., and Tueller, J. 1979, *Proc. 16th Internat. Cosmic-Ray Conf.* (Kyoto), **1**, 323.
Juliusson, E. 1974, *Ap. J.*, **191**, 331.
Koch-Miramond, L. 1981, *Proc. 17th Internat. Cosmic-Ray Conf.* (Paris), **12**, 21.
Koch-Miramond, L., Engelmann, J. J., Goret, P., Masse, P., Soutoul, A., Perron, C., Lund, N., and Rasmussen, I. L. 1983, *Proc. 18th Internat. Cosmic-Ray Conf.* (Bangalore), **2**, 219.
Letaw, J. 1983, *Ap. J. Suppl.*, **51**, 271.
Lezniak, J. A., and Webber, W. R. 1978, *Ap. J.*, **223**, 676.
Lindstrom, P. J., Greiner, D. E., Heckman, H. H., Cork, B., and Bieser, F. S. 1975, Lawrence Berkeley Laboratory preprint No. 3650.
Lund, N. 1985, in *Proc. Symposium on Nucleosynthesis and Acceleration of Cosmic Rays, COSPAR Advances in Space Exploration*, in press.
Mewaldt, R. A. 1981, *Proc. 17th Internat. Cosmic-Ray Conf.* (Paris), **13**, 49.
Mewaldt, R. A., Spalding, J. D., Stone, E. C., and Vogt, R. E. 1980, *Ap. J. (Letters)*, **236**, L121.
———. 1981, *Ap. J. (Letters)*, **251**, L27.
Meyer, J. P., Cassé, M., and Westergaard, N. 1975, *Proc. 14th Internat. Cosmic-Ray Conf.* (Munich), **12**, 4144.
Minagawa, G. 1981, *Ap. J.*, **248**, 847.
Ormes, J. F., and Protheroe, R. J. 1983, *Ap. J.*, **272**, 756.

Perron, C., *et al.* 1981, *Proc. 17th Internat. Cosmic-Ray Conf.* (Paris), **9**, 118.
Perron, C., and Koch, L. 1981, *Proc. 17th Internat. Cosmic-Ray Conf.* (Paris), **2**, 27.
Protheroe, R. J., Ormes, J. F., and Comstock, G. M. 1981, *Ap. J.*, **247**, 362.
Silberberg, R., and Tsao, C. H. 1973*a*, *Ap. J. Suppl.*, **25**, 315.
———. 1973*b*, *Ap. J. Suppl.*, **25**, 335.
———. 1977, *Proc. 15th Internat. Cosmic-Ray Conf.* (Plovdiv), **2**, 84.
Soutoul, A., Cassé, M., and Juliusson, E. 1978, *Ap. J.*, **219**, 753.
Tarlé, G., Ahlen, S. P., and Cartwright, B. G. 1979, *Ap. J.*, **230**, 607.
Tsao, C. H., and Silberberg, R. 1975, *Proc. 14th Internat. Cosmic-Ray Conf.* (Munich), **2**, 516.
———. 1979, *Proc. 16th Internat. Cosmic-Ray Conf.* (Kyoto), **2**, 202.
Webber, W. R. 1981, *Proc. 17th Internat. Cosmic-Ray Conf.* (Paris), **2**, 80.
Webber, W. R. 1982, *Ap. J.*, **255**, 329.
———. 1985, in *Proc. Symposium on Nucleosynthesis and Acceleration of Cosmic Rays, COSPAR Advances in Space Exploration*, in press.
Westfall, G. D., Wilson, L. W., Lindstrom, P. J., Crawford, H. C., Greiner, D. E., and Heckman, H. H. 1979, *Phys. Rev. C.*, **19**, 1309.
Wiedenbeck, M. E. 1985, in *Proc. Symposium on Nucleosynthesis and Acceleration of Cosmic Rays, COSPAR Advances in Space Exploration*, in press.
Wiedenbeck, M. E., Greiner, D. E., Bieser, F. S., Crawford, H. J., Heckman, H. H., and Lindstrom, P. J., 1979, *Proc. 16th Internat. Cosmic-Ray Conf.* (Kyoto), **1**, 412.
Young, J. S., Freier, P. S., Waddington, C. J., Brewster, N. R., and Fickle, R. K. 1981, *Ap. J.*, **246**, 1014.

ROBERT DWYER and PETER MEYER: Laboratory for Astrophysics and Space Research, Enrico Fermi Institute, University of Chicago, Chicago, IL 60637